Hindawi
Geofluids
Volume 2023, Article ID 3249570, 11 pages
https://doi.org/10.1155/2023/3249570

Research Article

Present-Day In Situ Stress Analysis in Shale Reservoir of Haiba Block, Southern Sichuan Basin, South China

Wei Guo,[1] Wei Ju,[2] Majia Zheng,[3] Weijun Shen,[4,5] Jian Zhang,[6] Pingping Liang,[1] Shengyu Wang,[2] and Haohao Hu[2]

[1]*Research Institute of Petroleum Exploration and Development, PetroChina, Beijing 100083, China*
[2]*School of Resources and Geosciences, China University of Mining and Technology, Xuzhou 221116, China*
[3]*PetroChina Southwest Oil and Gasfield Company, Chengdu 610000, China*
[4]*Key Laboratory for Mechanics in Fluid Solid Coupling Systems, Institute of Mechanics, Chinese Academy of Sciences, Beijing 100190, China*
[5]*School of Engineering Science, University of Chinese Academy of Sciences, Beijing 100049, China*
[6]*Shale Gas Institute, PetroChina Southwest Oil and Gasfield Company, Chengdu 610051, China*

Correspondence should be addressed to Weijun Shen; wjshen763@imech.ac.cn

Received 29 November 2021; Revised 1 August 2022; Accepted 6 October 2022; Published 22 February 2023

Academic Editor: Andrea Brogi

Natural gas from shale gas reservoirs has been an important contributor for reserve growth, deliverability construction, and profits growth in natural gas industry in the world. Hydraulic fracturing is commonly required in the shale gas commercial development, and thus understanding the present-day in situ stress field is greatly significant for the hydraulic fracturing and efficient development in shale gas reservoirs. However, there are no systematic investigations on the present-day in situ stress field in the Haiba Block from the Sichuan Basin, South China. In this study, the present-day in situ stress orientations and magnitudes in shale reservoir of Haiba Block are investigated based on the well interpretations from borehole image log and geomechanical modeling. Then, the effects of stresses on hydraulic fracturing, horizontal wells, and natural fracture reactivation were discussed. The results indicate that the horizontal maximum principal stress (S_{Hmax}) orientation is mainly in the NE-SW-trending, NW-SE-trending, and WNW-ESE-trending in the Haiba Block. The magnitudes of horizontal maximum and minimum principal stresses are 13.5 MPa~85.5 MPa and 2.8 MPa~31.6 MPa, respectively. In the Haiba Block, the differential stress is generally low in the northern part, which indicates that complex hydraulic fracture networks may be produced. While the natural fractures are generally stable under the present-day in situ stress field. When the increase of pore pressure gradient is about 30 KPa/m, nearly all natural fractures in the Longmaxi Formation may be reactivated. The results can provide the insights into a better understanding of the present-day in situ stress distribution so as to optimize perforation orientation, hydraulic fracturing design, and enhance gas production in shale gas reservoirs.

1. Introduction

With the deepening development of hydrocarbon exploration and development, unconventional hydrocarbon resources indicate the great effects on global energy structure, and among them, shale gas is an important and realistic alternative one [1–4]. Shale gas in the United States has been economical to produce for several years [5, 6]. According to a survey from the U.S. Energy Information Administration (EIA), nearly 75 percent of natural gas in the United States came from shale gas reservoirs in 2019 [7]. Shale gas resources are rich in China, and the EIA has showed that the technically recoverable shale gas reserves in China are 36.08×10^{12} m^3, which are the largest reserves in the world [8]. Therefore, speeding up the exploration and development of shale gas reservoirs is of greatly strategic significance for ensuring energy security and optimizing energy structure of natural gas in China.

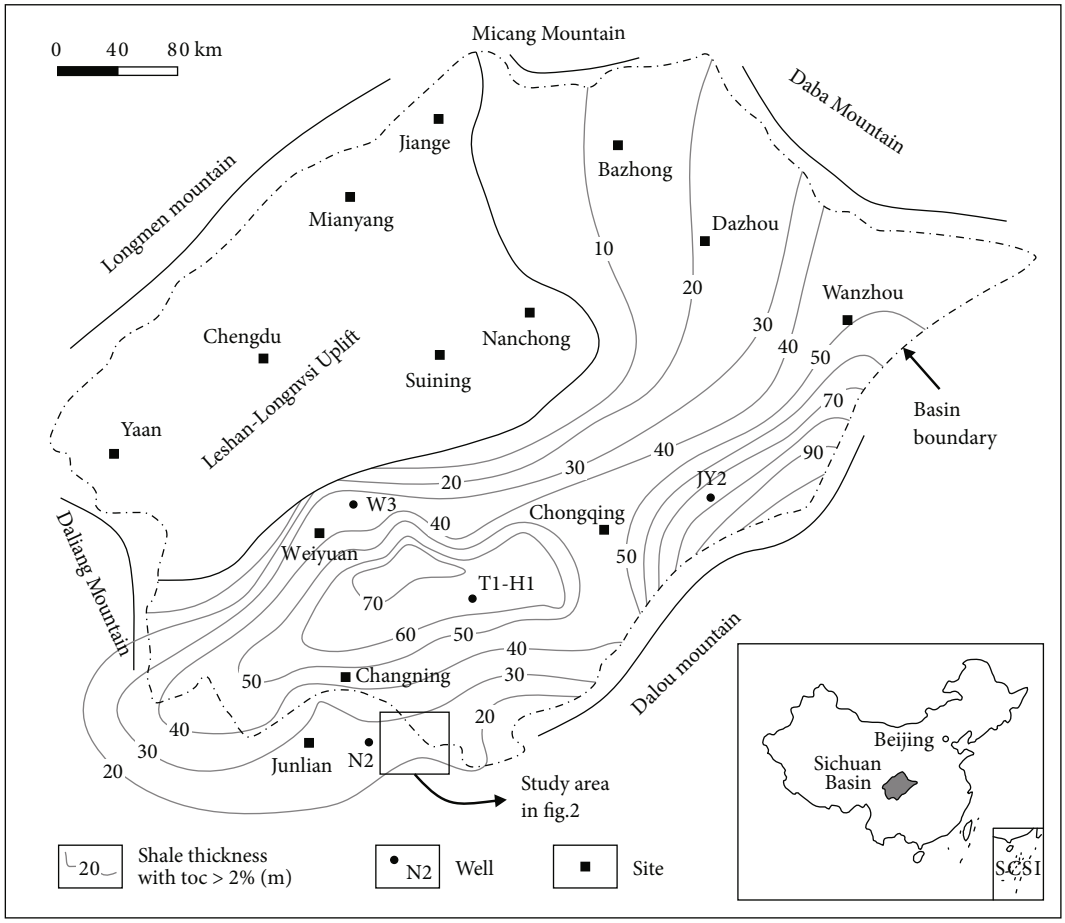

Figure 1: Geographic location and characteristics in the southern Sichuan Basin, China [17].

There are widely distributed marine shale gas resources in China, and shale gas exploration and development have achieved the remarkable success in the Sichuan Basin of China [9]. Within the basin, the Silurian Longmaxi Formation and Ordovician Wufeng Formation are characterized by the thick organic-rich shales and high thermal maturity. They are viewed as the most significant target layers for shale gas development, and the intensive exploration and exploitation are going currently [10–12]. Commonly, shale gas reservoirs are characterized by low porosity and low permeability, and the reservoir properties make the gas flow in shale pores difficult. The ability to economically produce natural gas from unconventional shale gas reservoirs has been made possible through the application of hydraulic fracturing and horizontal well drilling [6]. Knowledge of the present-day in situ stress state will help guide hydraulic fracturing design and greatly improve shale gas reservoir management [13, 14]. Consequently, understanding the present-day in situ stress distribution in shale gas reservoirs is essential to determine the mechanical characteristics of shale so as to provide the theoretical reference for hydraulic fracturing design and optimized perforation orientation in the shale gas exploitation and development.

In a sedimentary basin, the present-day in situ stress state may change both laterally and vertically. Generally, the description of present-day in situ stress state is based on vertical stress (S_v) magnitude, horizontal maximum principal stress (S_{Hmax}) magnitude, horizontal minimum principal stress (S_{hmin}) magnitude, and the orientation of S_{Hmax} [15]. According to the categorization from Jones [16], there exist three types of stress regime based on stress magnitude, including normal faulting stress regime ($S_v > S_{Hmax} > S_{hmin}$), strike-slip faulting stress regime ($S_{Hmax} > S_v > S_{hmin}$), and reverse faulting stress regime ($S_{Hmax} > S_{hmin} > S_v$). However, the Haiba Block of southern Sichuan Basin is a new shale gas exploration and development block in the Sichuan Basin, South China. Currently, there are few studies on the measured present-day in situ stress data and the scattered distributions, and a detailed understanding of the present-day in situ stress distribution in the shale gas reservoirs is lacking, which cannot support the further shale gas development. Hence, it is extremely necessary to understand in situ stress distribution so as to optimize perforation orientation and ultimately, hence, field production in shale gas reservoirs.

In this study, the present-day in situ stress states of the Haiba Block from the Sichuan Basin, South China were conducted using the finite element (FE) numerical simulations. The S_{Hmax} orientation was interpreted, and then the present-day in situ stress distribution in the Haiba Block was quantitatively delineated. Furthermore, the effects of stresses on hydraulic fracturing, horizontal wells, and natural

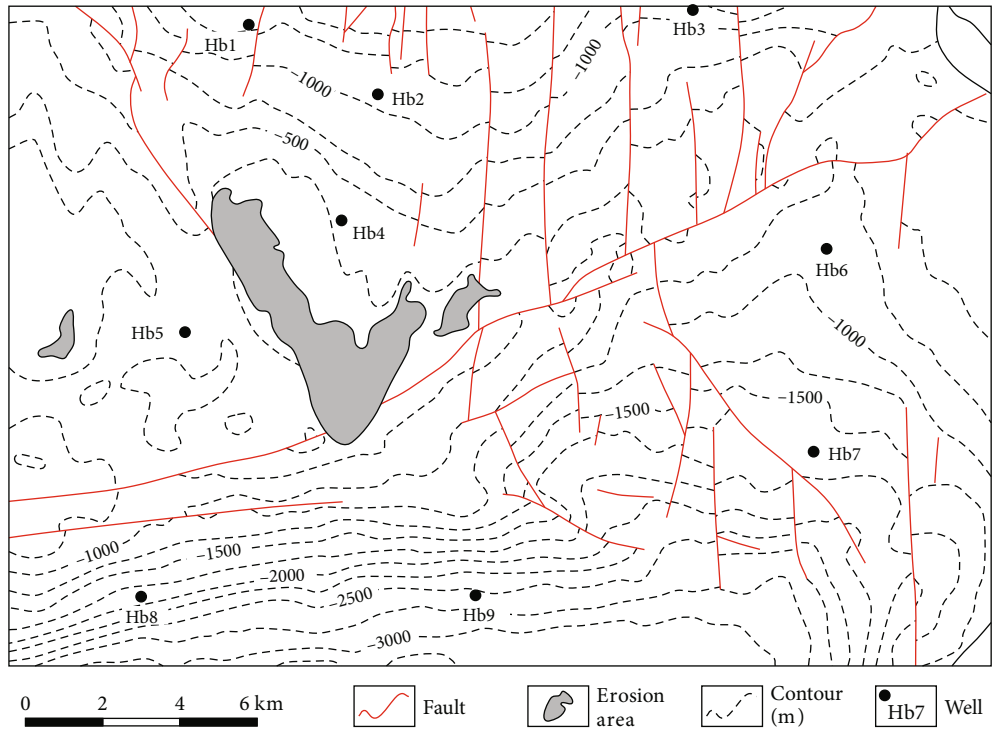

Figure 2: Structural framework of Haiba Block in the southern Sichuan Basin, China (The contours indicate the burial depth of bottom Wufeng Formation—Lower Silurian Longmaxi Formation).

fracture reactivation were analyzed to implicate gas production in shale gas reservoirs.

2. Geological Setting

The Sichuan Basin, a multiple-cycle diamond-shaped sedimentary basin, is located in the southwestern China, which is illustrated in Figure 1. The Basin covers an area of over $18 \times 104\,km^2$, which is an important area for shale gas commercial production in southern China [10, 17]. The Haiba Block is located in the southern portion of Sichuan Basin, which mainly includes the Haiba anticline, Yunshanba syncline, and Hualang syncline. The high-quality shale target is mainly developed in the Long 1 subformation, which is with a buried depth of 3000 m. During the past long geological evolution, the Haiba Block experienced the multiple phases of tectonic activities, and which resulted in a series of well-developed faults as shown in Figure 2.

In the Haiba Block, the Wufeng Formation and Longmaxi Formation are the most important layers for shale gas development, whose lithology is characterized by black carbonaceous/silty shale and mudstone as illustrated in Figure 3. The Longmaxi Formation can be divided into two subformation (Long 1 and Long 2), and Long 1 subformation is further divided into two segments: Long 1^1 and Long 1^2 from bottom to top. Burial depths of the Wufeng Formation are distributed from 600 m to 1500 m as shown in Figure 2. The thickness of Wufeng Formation and Longmaxi Formation is generally stable within the Haiba Block, which varies in the intervals of 4 ~ 15 m and 200 ~ 250 m, respectively. As shown in Figure 3, the experiment results show that the porosity of Wufeng-Longmaxi Formations varies between 2.78% and 7.89% with an average of 4.7%, and the TOC ranges from 1.02% to 6.06% with an average of 3.0%. The well tests indicate that the Wufeng Formation and Longmaxi Formation Long 1^1 segment is the target production layer for shale gas of the Haiba Block in the southern Sichuan Basin, South China.

3. Interpretation of the S_{Hmax} Orientation

In general, wellbore breakouts (WBs), drilling-induced tensile fractures (DITFs), earthquake focal mechanisms, in situ stress measurements, etc., could be used as the important stress indicators to determine the S_{Hmax} orientation [18, 19]. Commonly, both WBs and DITFs could be detected from the borehole image log, as illustrated in Figure 4. The WBs orientation indicates the azimuth of S_{hmin}, perpendicular to the S_{Hmax} orientation [13, 20]. However, the directions of the DITFs are indicative of the S_{Hmax} orientations [21]. In borehole image log, the DITFs usually appear in two different patterns. One pattern is the symmetrically aligned fractures parallel or subparallel to borehole axis on the opposite sides of the borehole wall, as shown in Figure 4(a). The other pattern is the en echelon fractures around the borehole showing traces 180° apart, as illustrated in Figure 4(b). The WBs are commonly shown as broad, parallel conductive zones separated by approximately 180° in borehole image log, which are shown in Figure 4(c).

In this study, based on available data in the Haiba Block, the interpretations of the S_{Hmax} orientation are mainly carried out in wells Hb1, Hb2, Hb3, Hb4, Hb5, and Hb7 from

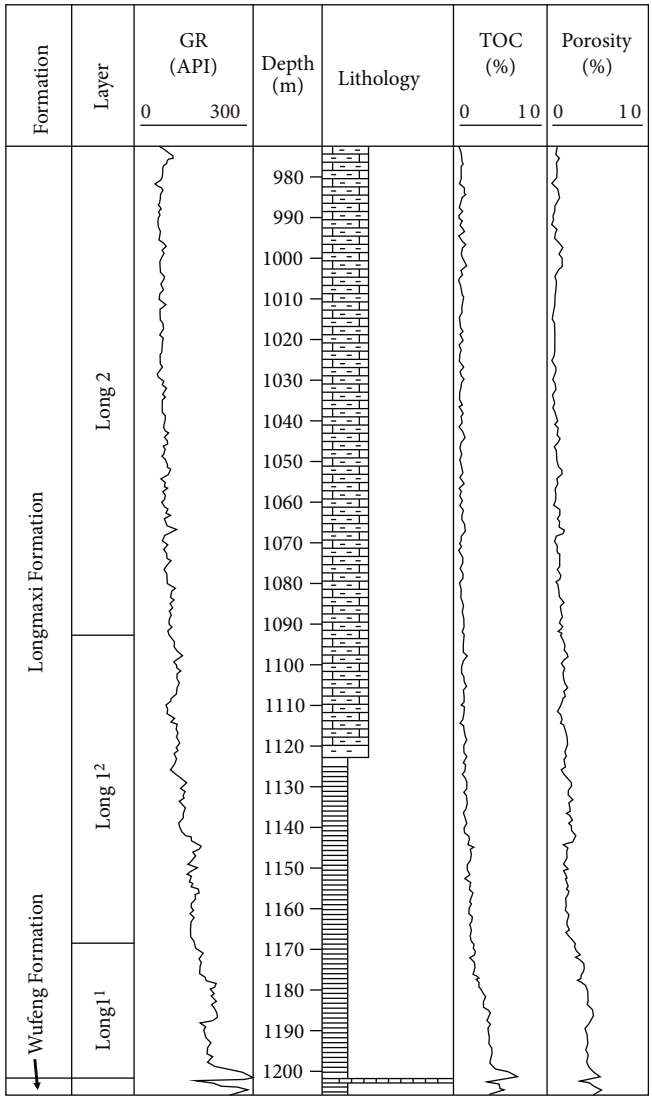

Figure 3: Typical lithological system of the Wufeng Formation and Longmaxi Formation in the Haiba Block (Well Hb3).

the stress indicators of WBs and DITFs, separately. The results show that the S_{Hmax} orientations in the Wufeng-Longmaxi Formations of Haiba Block mainly indicate the NE-SW-trending, NW-SE-trending, and WNW-ESE-trending as illustrated in Figure 5. According to the tectonic analysis in a larger scale, the NE-SW-trending may be a regional S_{Hmax} orientation. The NW-SE-trending and WNW-ESE-trending are the local S_{Hmax} orientations. The development of faults and natural fractures, lateral lithology differences, etc., could function as the important factors influencing variations of the S_{Hmax} orientations in the Haiba Block.

4. Present-Day In Situ Stress Prediction

In the Haiba Block, the measured in situ stress magnitudes are few and widely spread. Consequently, the overall characteristics of present-day stress distribution in the Haiba Block cannot be fully understood. In this study, the detailed in situ stress distributions in the Haiba shale reservoirs are delineated according to the finite element (FE) numerical method. Generally, the basic principles and procedures for the FE stress simulation are as follows: (1) a complete geological model is established and further discretized into a finite number of elements connected by the nodes; (2) the corresponding rock mechanics parameters are assigned to those elements divided; (3) the continuous stress function and strain function of the geological body are transformed into a field function for solving finite points, which is used by the following:

$$\sigma = \left[\sigma_x\, \sigma_y\, \sigma_z\, \tau_{xy}\, \tau_{yz}\, \tau_{zx}\right]^T, \tag{1}$$

$$\varepsilon = \left[\varepsilon_x\, \varepsilon_y\, \varepsilon_z\, \gamma_{xy}\, \gamma_{yz}\, \gamma_{zx}\right]^T, \tag{2}$$

$$\sigma = D\varepsilon, \tag{3}$$

$$[P] = [K][\delta], \tag{4}$$

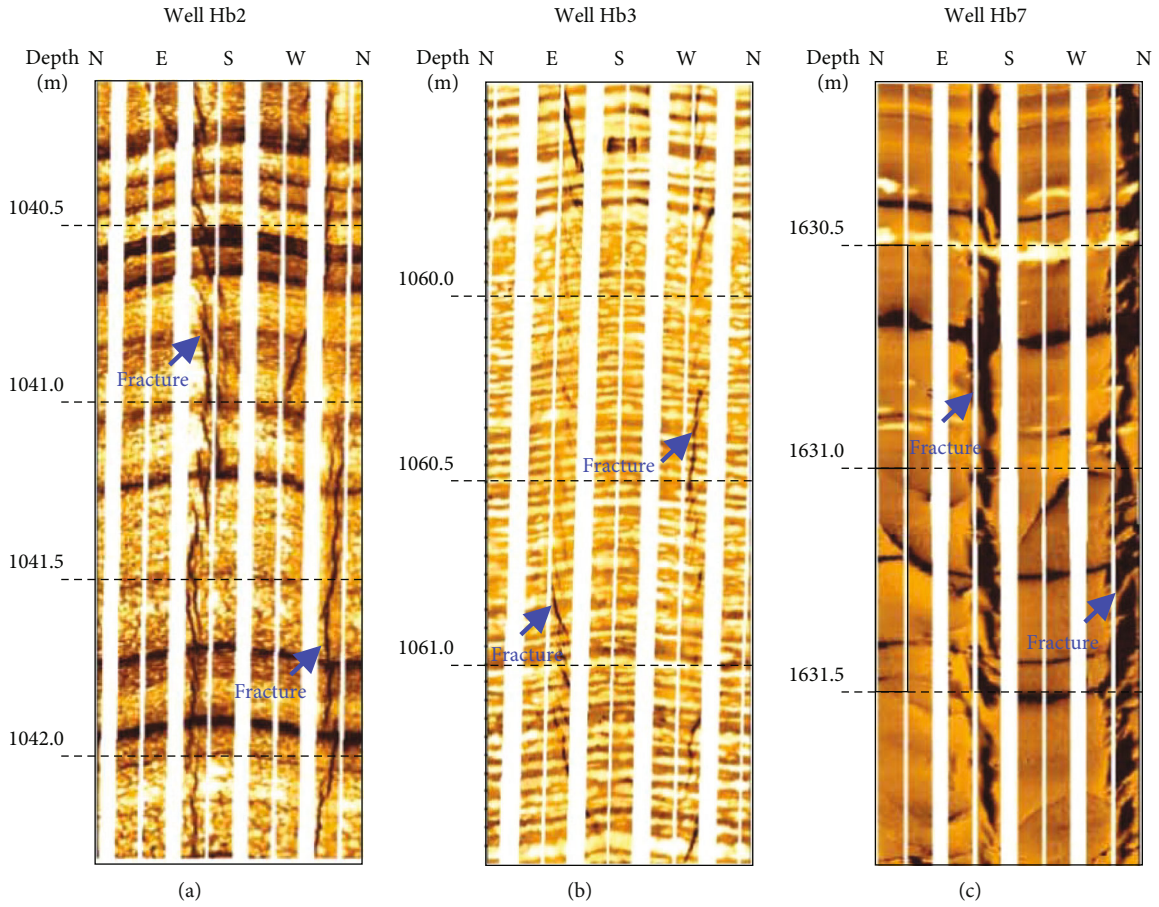

Figure 4: Borehole image logs showing drilling-induced tensile fractures (DITFs) and wellbore breakouts (WBs) in the Haiba Block.

where σ is the stress; ε is the strain; D is the elastic matrix; $[P]$ is the integral nodal load matrix; $[K]$ is the integral stiffness matrix; and $[\delta]$ is the nodal displacement matrix for the integral structure of the examined elemental array.

By solving the linear equation, the nodal displacement, strain, and stress of each individual element in the structure can be determined [22].

Generally, the fracture closure pressure (P_c) is indicative of the S_{hmin} magnitude at the test depth, which can be described as follows [23, 24],

$$S_{hmin} = P_c, \tag{5}$$

According to the previous studies [25], the S_{Hmax} magnitude is generally calculated and expressed as follows:

$$S_{hmax} = 3S_{hmin} - P_f - P_o + T, \tag{6}$$

where P_f is the formation break-down pressure; P_o is the pore pressure; and T is the tensile strength of the rock.

4.1. Geological Model Setup. The accuracy of the geological model directly determines the credibility of the in situ stress simulation results [26, 27]. In this study, the Silurian Longmaxi Formation of Haiba Block, southern Sichuan Basin, South China is selected for the model setup and further

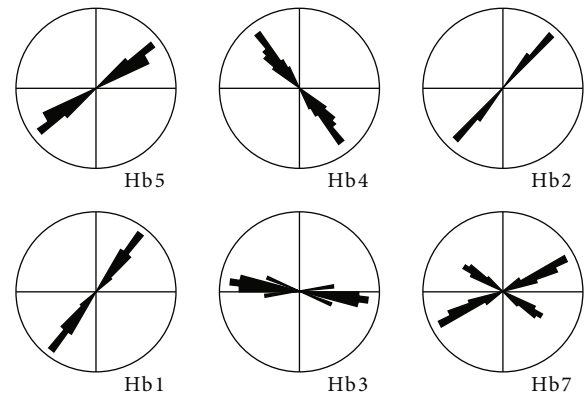

Figure 5: The S_{Hmax} orientations interpreted from drilling-induced tensile fractures (DITFs) and wellbore breakouts (WBs) in the Haiba Block.

stress analysis. The initial three-dimentional (3D) geometric model is constructed based on the structural and sedimentary conditions in the Haiba Block as shown in Figure 6. According to the principals of the finite element method, the faults are generally represented by the zones inside the model [28], which is illustrated in Figure 6(a). Consequently, the constructed 3D geometric model contains different zones representing the geological units, namely, the Longmaxi Formation and faults.

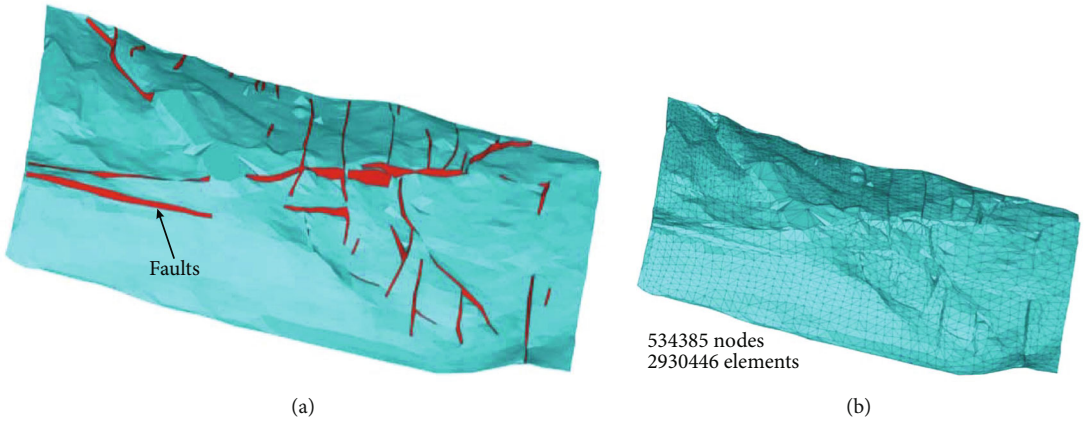

Figure 6: Geometry (a) and meshing results (b) of the initial Haiba 3D model.

Table 1: Reservoir rock mechanics parameters used in this study.

Unit	Density ρ (kg/m^3)	Young's modulus E (GPa)	Poisson's ratio μ
Target layer	2500	25.0	0.23
Fault zone	1750	17.5	0.25
Nested model	2550	27.0	0.25

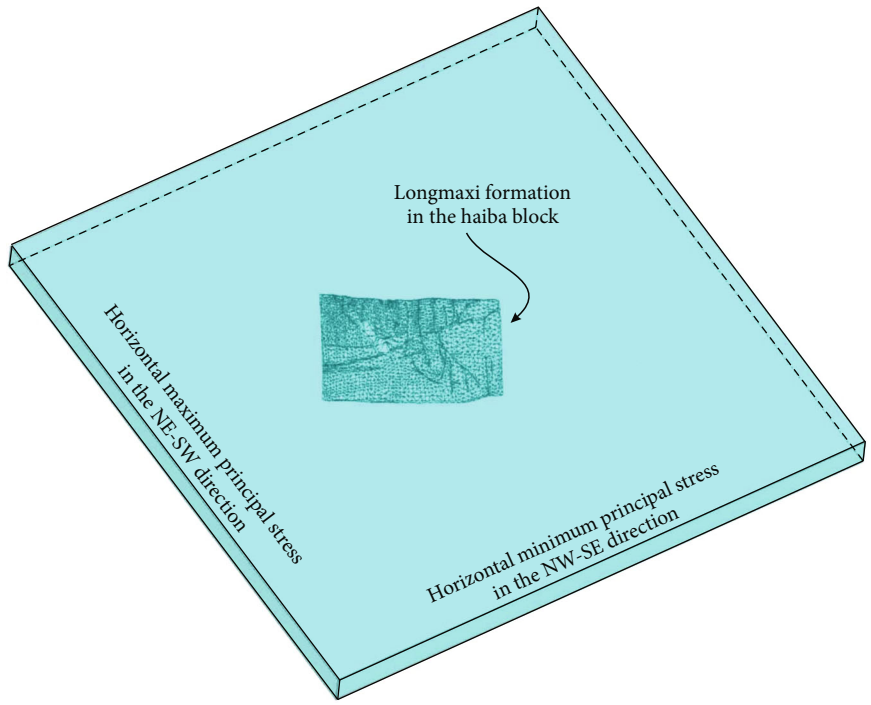

Figure 7: Simplified nested model of the Longmaxi Formation in the Haiba Block.

In the following, the reservoir properties are assigned to these different units to make into the geological model. In this study, the mechanical parameters of the target layer (Longmaxi Formation) are determined by the rock mechanics experiments. They are the average values obtained from 20 samples, and the rock mechanics parameters used in this study are listed in Table 1. In addition, the faults are developed in the study area, and their distribution can largely influence the in situ stresses. However, within the FE model, the mechanics parameters for fault zones are unavailable from the laboratory experiments. As to this question, the faults in the FE models are generally defined as the weakness zones with their Young's moduli lower than the corresponding sedimentary layer. The Young's modulus ratio between

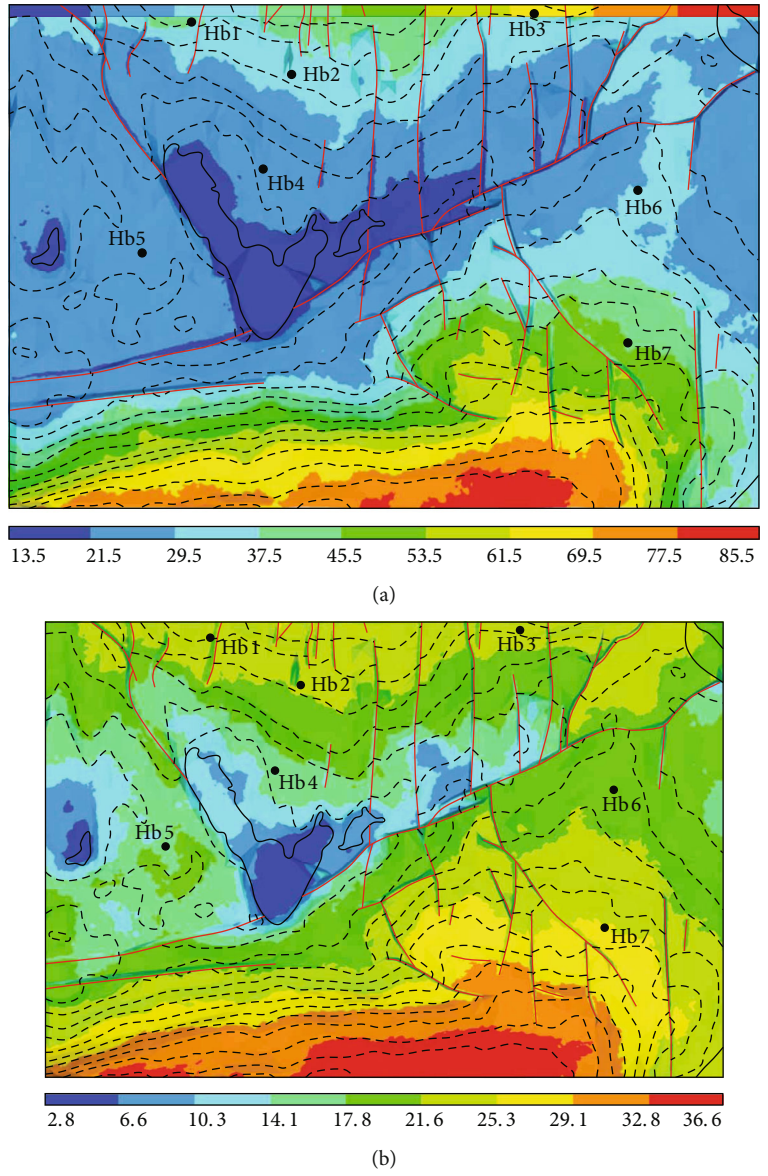

FIGURE 8: The calculated S_{Hmax} (a) and S_{hmin} (b) magnitudes in the Longmaxi Formation of Haiba Block (compressive stresses are considered as positive and tensile stresses are negative).

fault zone and sedimentary layer is commonly between 0.5 and 0.7 [26, 29], and a ratio of 0.7 is used in this study. All faults and sedimentary layers in this model are meshed or discretized using primarily three-nodel triangular elements. After the meshing, approximately 534385 nodes and 2930446 elements are produced within the FE model as illustrated in Figure 6(b).

4.2. Boundary Conditions. In this study, the boundary conditions are difficult to determine and apply because there is no clear geological boundary to demarcate the Haiba Block from the rest parts of Sichuan Basin. To solve this problem and facilitate the applying forces, the Haiba Block is nested within a larger rectangular parallelepiped approximately 5 times of the study area, as illustrated in Figure 7. Vertically, the entire geological model is subjected to the gravity loading ($g = 9.8\,m/s^2$), which can be directly and automatically applied in the finite element software. Laterally, according to the measured stress data and several attempts, the stress magnitudes of approximately $S_{Hmax} = 32$ MPa and $S_{hmin} = 27$ MPa are used in the NE-SW direction and NW-SE direction of the nested model, respectively. In addition, some appropriate displacement constraints are applied to the geological model so as to prevent it from the rotation and rigid displacement. The top of the model is set as a free surface, and the bottom is vertically fixed. In the numerical analysis, the stress symbols are defined based on the following rules that compressive stresses are positive and tensile stresses are negative. In the following, the node displacement is taken as the objective function to build the multivariate equations, and the stress and strain values in each element body are calculated [27].

Table 2: Error analysis of the measured and calculated stress results from numerical simulation.

Well	Measured S_{Hmax} (MPa)	Calculated S_{Hmax} (GPa)	Error (%)	Measured S_{hmin} (MPa)	Calculated S_{hmin} (MPa)	Error (%)
Hb1	38.6	39.6	2.59	24.7	23.1	6.48
Hb2	30.1	32.6	8.31	19.7	21.5	9.14
Hb3	35.9	37.9	5.57	22.5	23.9	6.22
Hb4	14.7	22.1	50.34	11.1	14.5	30.63
Hb7	53.1	49.5	6.78	30.3	26.8	11.55

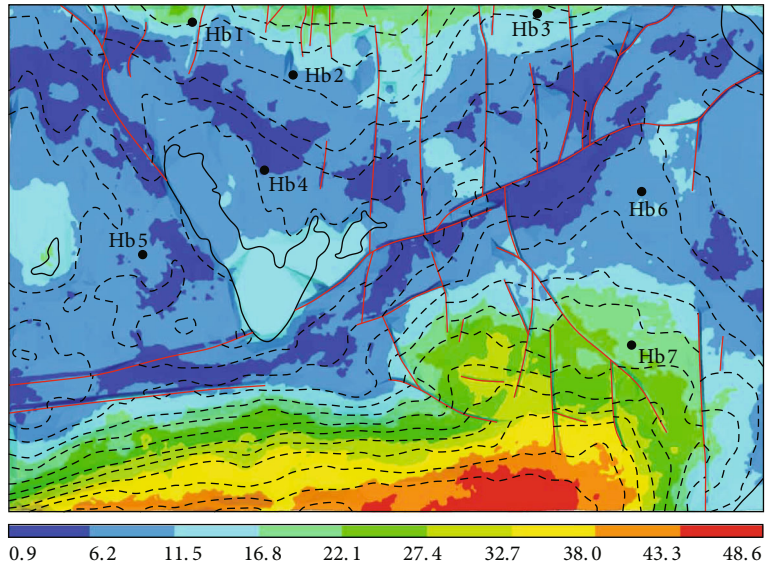

Figure 9: Differential stress in the Longmaxi Formation of Haiba Block Stress (unit: MPa).

4.3. Results and Error Analysis. In the Longmaxi Formation of Haiba Block, southern Sichuan Basin, the S_{Hmax} values range from 13.5 MPa to 85.5 MPa as illustrated in Figure 8(a), and the S_{hmin} values are between 2.8 MPa and 36.6 MPa as shown in Figure 8(b), both of which are the indicative of compression. The calculated results indicate that the stress distributions in the study area are greatly depth- and fault-controlled, i.e., faults and burial depth greatly influence the present-day stress distribution. The lower stress magnitudes are mainly distributed in regions around wells Hsb5-Hb6 and fault zones.

In order to verify the credibility of the calculated stress results shown in Figure 8, and the error analysis is described based on the following:

$$r = \frac{|d1 - d2|}{d2} \times 100\%, \quad (7)$$

where r is the error between the calculated and measured stress values and $d1$ and $d2$ are the calculated and measured stress values, respectively.

In this study, the errors between the measured and calculated stress magnitudes are low, and they are generally less than 12% except Well Hb4, which is listed in Table 2. It implies that this modeling results are believable, and there are two reasons for the relatively high error between the measured and calculated stress values in Well Hb4. One reason is that the error calculated based on Equation (4) may be larger when the absolute stress magnitudes are relatively low. The other reason is that Well Hb4 is located around the erosion areas, and the erosion effects on stress magnitude are not taken into account in the simulation process. In general, the predicted stress distribution shown in Figure 8 may provide the geological references for further shale gas exploration and development.

5. Implications for Shale Gas Production

5.1. Effects of Stresses on Hydraulic Fracturing and Horizontal Wells. The growth in shale gas production in the United States and other countries has been a direct consequence of utilizing hydraulic fracturing and drilling horizontal wells, which creates a complex fracture network allowing for the gas improvement during well performance [30, 31]. And thus the hydraulic fracturing and horizontal wells are required in the commercial development of shale gas. The present-day in situ stress state indicates the critical effects on hydraulic fracturing operations and horizontal well drillings.

Differential stress is an important factor during the hydraulic fracturing design, and the lower differential stress magnitude commonly results in complex fracture networks [32, 33]. In this study, based on the present-day stress prediction results, differential stress magnitudes in the Longmaxi Formation of Haiba Block vary between 0.9 MPa and 48.6 MPa, which are mainly controlled by the burial depth

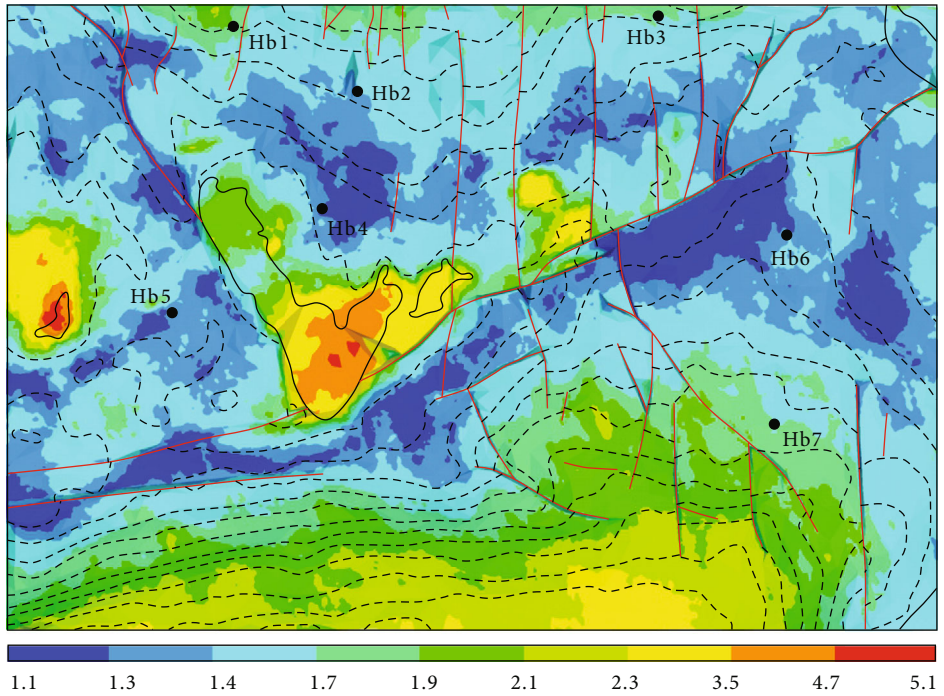

Figure 10: Distribution of the unequilibrium tectonic indicator (K) in the Longmaxi Formation of Haiba Block.

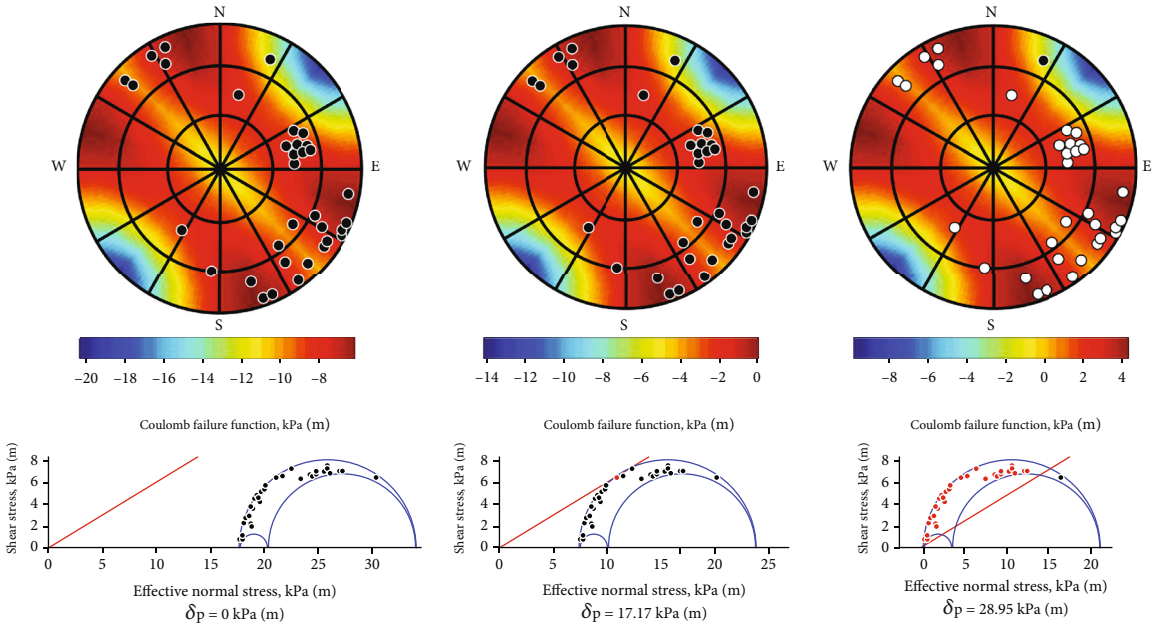

Figure 11: Lower hemisphere stereonet plots and Mohr's circles analyzing natural fracture reactivation risks in Well Hb2 of Haiba Block.

as illustrated in Figure 9. In the northern part (structurally high areas), differential stress magnitudes are generally low, and they are less than 11.5 MPa. However, with the increasing burial depth in the southern part, differential stress magnitudes are high, and they are generally higher than 22.1 MPa. Consequently, it can be deduced that the complex hydraulic fracture networks will be produced in the northern part of Haiba Block.

The unequilibrium tectonic indicator (K), a ratio between S_{Hmax} magnitude and S_{hmin} magnitude, is a significant factor in hydraulic fracturing design [27]. In this study, the K value ranges between 1.1 and 5.1 in the Longmaxi Fromation as shown in Figure 10. Based on the results both in Figures 9 and 10, the areas with low differential stress and K are the engineering sweet spots for subsequent shale gas development in the Haiba Block. In addition, drilling horizontal well is the other important and critical technique for shale gas production. Commonly, a newly generated hydraulic fracture generally propagates along the path that requires the minimum force [30, 34]. Therefore, in the Longmaxi

shale reservoir of Haiba Block, horizontal wells are better drilled parallel to the S_{hmin} direction as shown in Figure 5.

5.2. Effects of Stresses on Natural Fracture Reactivation. In general, during the hydraulic fracturing within shale gas reservoir, fluids are injected into the target subsurface reservoir rocks, resulting in geomechanically-induced effects, such as natural fracture reactivation [3, 34]. In this study, the reactivation risk plots are introduced to analyze natural fracture reactivations, which use the Mohr's circle criterion [35]. Natural fractures within the Longmaxi Formation of Well Hb2 are selected as the example for analysis. The plots are shown in Figure 11 with warm and cold colors, which indicate higher and lower fracture reactivation risk, respectively.

In the Haiba Block, initially, the failure line (red line) is far from Mohr's circle, which indicates all natural fractures are stable under the present stress field. When fluids are injected into the target shale gas reservoir, the Mohr's circle moves left as illustrated in Figure 11, which increases the reactivation risk for natural fractures. Fractures are in their critical state when the failure line rightly gets into contact with the Mohr's circle. In this study, based on the modeling analysis, when the pore pressure gradient caused by fluid injection increases 28.95 kPa/m, nearly all natural fractures in the Longmaxi Formation of Well Hb2 are reactivated as shown in Figure 11. The fracture orientations are plotted as the pole of planes with different colors representing the relative ease of fracture susceptibility as the amount of pore pressure increase required to reactivate a fracture. The red colors show the highest likelihood of the fracture reactivation, while the blue colors indicate the least likelihood of reactivation for all possible fractures in the present-day stress state. The black and white dots in the stereonet plots are normal and critically stressed natural fractures, respectively. In the Mohr circles, the black and red dots are normal and critically stressed natural fractures, and the δp indicates the pore pressure increases.

6. Conclusions

Accurate knowledge of the present-day in situ stress field can help shale gas exploration and development of the Haiba Block in the Sichuan Basin, South China. In this study, the present-day in situ stress distribution and orientations are analyzed based on the numerical simulation and interpretations from borehole image log. And then the effects of stresses on hydraulic fracturing, horizontal wells, and natural fracture reactivation were discussed to illustrate gas production in shale gas reservoirs. The main conclusions are as follows. (1) The S_{Hmax} orientations in the Wufeng-Longmaxi shale reservoirs of Haiba Block are mainly the NE-SW-trending, NW-SE-trending, and WNW-ESE-trending, and the NE-SW-trending is the regional S_{Hmax} direction. In the Longmaxi Formation, the S_{Hmax} values range from 13.5 MPa to 85.5 MPa, while the S_{hmin} values are between 2.8 MPa and 36.6 MPa, and they are indicative of the compression. The distributions of stress magnitudes in the study area are greatly depth- and fault-controlled, and the deeper depths (e.g., the southern part of Haiba Block) indicate the larger in situ stress magnitudes. (2) In the Haiba Block, the differential stress is generally low in the northern part and high in southern part, which indicates that the complex hydraulic fracture networks will be produced in the northern part of Haiba Block. In addition, based on natural fracture reactivation analysis, all natural fractures are initially stable under the present-day stress field. When the increase of pore pressure gradient is approximately 30 kPa/m, nearly all natural fractures in the Longmaxi Formation will be reactivated.

Data Availability

The data used to support the findings of this study are included within the article.

Conflicts of Interest

The authors declared no potential conflicts of interest with respect to the research, authorship, and publication of this article.

Acknowledgments

This work was supported by the National Key Research and Development Project (2020YFA0711800) and by the National Natural Science Foundation of China (NO. 12172362 and NO. 41971335). We also thank the support by the Natural Science Foundation of Jiangsu Province, China (BK20201349).

References

[1] D. M. Jarvie, R. J. Hill, T. E. Ruble, and R. M. Pollastro, "Unconventional shale-gas systems: the Mississippian Barnett Shale of North-Central Texas as one model for thermogenic shale-gas assessment," *AAPG Bulletin*, vol. 91, no. 4, pp. 475–499, 2007.

[2] W. J. Shen, T. R. Ma, X. Z. Li, B. Sun, Y. Hu, and J. Xu, "Fully coupled modeling of two-phase fluid flow and geomechanics in ultra-deep natural gas reservoirs," *Physics of Fluids*, vol. 34, no. 4, article 043101, 2022.

[3] W. Ju, X. B. Niu, S. B. Feng et al., "Present-day in-situs stress field within the Yanchang Formation tight oil reservoir of Ordos Basin, Central China," *Journal of Petroleum Science and Engineering*, vol. 187, article 106809, 2020.

[4] W. J. Shen, X. Z. Li, T. R. Ma, J. Cai, X. Lu, and S. Zhou, "High-pressure methane adsorption behavior on deep shales: experiments and modeling," *Physics of Fluids*, vol. 33, no. 6, article 063103, 2021.

[5] K. A. Bowker, "Barnett shale gas production, Fort Worth Basin: issues and discussion," *AAPG Bulletin*, vol. 91, no. 4, pp. 523–533, 2007.

[6] D. Rahm, "Regulating hydraulic fracturing in shale gas plays: the case of Texas," *Energy Policy*, vol. 39, no. 5, pp. 2974–2981, 2011.

[7] X. H. Ma, W. J. Shen, X. Z. Li, Y. Hu, X. Liu, and X. Lu, "Experimental investigation on water adsorption and desorption isotherms of the Longmaxi shale in the Sichuan Basin, China," *Scientific Reports*, vol. 10, no. 1, p. 13434, 2020.

[8] X. Z. Li, Z. H. Guo, Y. Hu et al., "High-quality development of ultra-deep large gas fields in China: challenges, strategies and

proposals," *Natural Gas Industry*, vol. 7, no. 5, pp. 505–513, 2020.

[9] X. L. Tang, Z. X. Jiang, S. Jiang et al., "Characteristics, capability, and origin of shale gas desorption of the Longmaxi Formation in the southeastern Sichuan Basin, China," *Scientific Reports*, vol. 9, no. 1, p. 1035, 2019.

[10] C. N. Zou, Z. Yang, J. X. Dai et al., "The characteristics and significance of conventional and unconventional Sinian-Silurian gas systems in the Sichuan Basin, Central China," *Marine and Petroleum Geology*, vol. 64, pp. 386–402, 2015.

[11] W. Ju, J. L. Wang, H. H. Fang, Y. Gong, and S. Zhang, "Paleostress reconstructions and stress regimes in the Nanchuan region of Sichuan Basin, South China: implications for hydrocarbon exploration," *Geosciences Journal*, vol. 21, no. 4, pp. 553–564, 2017.

[12] W. J. Shen, X. Z. Li, Y. M. Xu, Y. Sun, and W. Huang, "Gas flow behavior of nanoscale pores in shale gas reservoirs," *Energies*, vol. 10, no. 6, p. 751, 2017.

[13] M. D. Zoback, C. A. Barton, M. Brudy et al., "Determination of stress orientation and magnitude in deep wells," *International Journal of Rock Mechanics and Mining Sciences*, vol. 40, no. 7-8, pp. 1049–1076, 2003.

[14] M. Tingay, R. R. Hillis, C. K. Morley, R. C. King, R. E. Swarbrick, and A. R. Damit, "Present-day stress and neotectonics of Brunei: implications for petroleum exploration and production," *AAPG Bulletin*, vol. 93, no. 1, pp. 75–100, 2009.

[15] M. Rajabi, M. Tingay, and O. Heidbach, "The present-day state of tectonic stress in the Darling Basin, Australia: implications for exploration and production," *Marine and Petroleum Geology*, vol. 77, pp. 776–790, 2016.

[16] O. Jones, "The Dynamics of faulting and dyke formation: with applications to Britain," *Nature*, vol. 149, no. 3789, pp. 651-652, 1942.

[17] Q. Z. Guan, D. Z. Dong, S. F. Wang et al., "Preliminary study on shale gas microreservoir characteristics of the lower Silurian Longmaxi Formation in the southern Sichuan Basin, China," *Journal of Natural Gas Science and Engineering*, vol. 31, pp. 382–395, 2016.

[18] O. Heidbach, M. Tingay, A. Barth, J. Reinecker, D. Kurfeß, and B. Müller, "Global crustal stress pattern based on the World Stress Map database release 2008," *Tectonophysics*, vol. 482, no. 1-4, pp. 3–15, 2010.

[19] W. Ju, Z. L. Li, W. F. Sun, and H. Xu, "In-situ stress orientations in the Xiagou tight oil reservoir of Qingxi oilfield, Jiuxi Basin, Northwestern China," *Marine and Petroleum Geology*, vol. 98, pp. 258–269, 2018.

[20] J. D. O. Williams, M. W. Fellgett, A. Kingdon, and J. P. Williamson, "In-situ stress orientations in the UK Southern North Sea: regional trends, deviations and detachment of the post-Zechstein stress field," *Marine and Petroleum Geology*, vol. 67, pp. 769–784, 2015.

[21] M. Sandiford, M. Wallace, and D. Coblentz, "Origin of the in situ stress field in South-Eastern Australia," *Basin Research*, vol. 16, no. 3, pp. 325–338, 2004.

[22] W. Zeng, W. Ding, J. Zhang et al., "Fracture development in Paleozoic shale of Chongqing area (South China). Part two: numerical simulation of tectonic stress field and prediction of fractures distribution," *Journal of Asian Earth Sciences*, vol. 75, pp. 267–279, 2013.

[23] A. J. White, M. O. Traugott, and R. E. Swarbrick, "The use of leak-off tests as means of predicting minimumin-situstress," *Petroleum Geoscience*, vol. 8, no. 2, pp. 189–193, 2002.

[24] R. Liu, J. Z. Liu, W. L. Zhu et al., "In situ stress analysis in the Yinggehai Basin, northwestern South China Sea: implication for the pore pressure-stress coupling process," *Marine and Petroleum Geology*, vol. 77, pp. 341–352, 2016.

[25] M. K. Hubbert and D. G. Willis, "Mechanics of hydraulic fracturing," *AIME Petroleum Transactions*, vol. 210, no. 1, pp. 153–168, 1957.

[26] W. Ju and W. F. Sun, "Tectonic fractures in the lower Cretaceous Xiagou Formation of Qingxi oilfield, Jiuxi Basin, NW China. Part two: numerical simulation of tectonic stress field and prediction of tectonic fractures," *Journal of Petroleum Science and Engineering*, vol. 146, pp. 626–636, 2016.

[27] J. S. Liu, H. M. Yang, X. F. Wu, and Y. Liu, "The in situ stress field and microscale controlling factors in the Ordos Basin, Central China," *International Journal of Rock Mechanics and Mining Sciences*, vol. 135, no. 7, article 104482, 2020.

[28] K. Fischer and A. Henk, "A workflow for building and calibrating 3-D geomechanical models–a case study for a gas reservoir in the North German Basin," *Solid Earth*, vol. 4, no. 2, pp. 347–355, 2013.

[29] K. Jiu, W. L. Ding, W. H. Huang, S. You, Y. Zhang, and W. Zeng, "Simulation of paleotectonic stress fields within Paleogene shale reservoirs and prediction of favorable zones for fracture development within the Zhanhua depression, Bohai Bay Basin, East China," *Journal of Petroleum Science and Engineering*, vol. 110, pp. 119–131, 2013.

[30] A. Kingdon, M. W. Fellgett, and J. D. O. Williams, "Use of borehole imaging to improve understanding of the in-situ stress orientation of central and Northern England and its implications for unconventional hydrocarbon resources," *Marine and Petroleum Geology*, vol. 73, pp. 1–20, 2016.

[31] M. H. Rmmay and A. A. Awotunde, "Stochastic optimization of hydraulic fracture and horizontal well parameters in shale gas reservoirs," *Journal of Natural Gas Science and Engineering*, vol. 36, pp. 71–78, 2016.

[32] A. N. Dehghan, K. Goshtasbi, K. Ahangari, and Y. Jin, "Experimental investigation of hydraulic fracture propagation in fractured blocks," *Bulletin of Engineering Geology and the Environment*, vol. 74, no. 3, pp. 887–895, 2015.

[33] Y. S. Zhang, J. C. Zhang, B. Yuan, and S. Yin, "In-situ stresses controlling hydraulic fracture propagation and fracture breakdown pressure," *Journal of Petroleum Science and Engineering*, vol. 164, pp. 164–173, 2018.

[34] S. Reynolds, R. Hillis, and E. Paraschivoiu, "In situ stress field, fault reactivation and seal integrity in the Bight Basin, South Australia," *Exploration Geophysics*, vol. 34, no. 3, pp. 174–181, 2003.

[35] S. D. Mildren, R. R. Hillis, and J. Kaldi, "alibrating predictions of fault seal reactivation in the Timor Sea," *Journal of the Australian Petroleum Production & Exploration Association*, vol. 42, no. 1, pp. 187–202, 2002.